Automated detection of diabetic foot with and without neuropathy using double density-dual tree-complex wavelet transform on foot thermograms

Muhammad Adam[1*], Eddie Y K Ng[2], Shu Lih Oh[1], Marabelle L. Heng[5], Yuki Hagiwara[1], Jen Hong Tan [1], Jasper W.K. Tong[6], U Rajendra Acharya[1,3,4]

[1]Department of Electronics and Computer Engineering, Ngee Ann Polytechnic, Singapore.
[2]School of Mechanical and Aerospace Engineering, Nanyang Technological University, Singapore.
[3]Department of Biomedical Engineering, School of Science and Technology, SIM University, Singapore.
[4]Department of Biomedical Engineering, Faculty of Engineering, University of Malaya, Malaysia.
[5]Podiatry Department, Singapore General Hospital.
[6]Allied Health Office, KK Women's and Children's Hospital.

*Corresponding Author
Postal Address: [1]Department of Electronics and Computer Engineering, Ngee Ann Polytechnic, Singapore 599489
Telephone: +65-64607887; Email Address: muhdadam@hotmail.com

ABSTRACT

Diabetic foot is ~~a~~ the most common problem among diabetic patients, mainly due to peripheral vascular and neuropathy induced capillary perfusion changes. These pathogenic factors cause superficial temperature changes that can be qualitatively and visually documented using infrared thermography (IRT). Hence, ~~the~~ IRT can potentially be used to ~~detect~~ evaluate the diabetic foot. However, it is tedious to manually interpret these subtle temperature variations by inspecting the foot image. Therefore, an automated system to detect diabetic foot with and without neuropathy is proposed. In this study, 51 healthy individuals and 66 diabetic patients (33 with and 33 without neuropathy) are

considered. The plantar foot thermograms are decomposed into coefficients using double density-dual tree-complex wavelet transform (DD-DT-CWT). Several entropy and texture features are extracted from the decomposed images of left, right and bilateral foot. These features are reduced using various dimensionality reduction techniques and subsequently ranked using *F*-values. The ranked features are fed individually into the different classifiers one by one. The developed system yielded 93.16% accuracy[IIA1], 90.91% sensitivity and 98.04% specificity using only *four* locality sensitive discriminant analysis (LSDA) features obtained from both (left and right) foot thermograms with k-nearest neighbour (kNN) classifier. This automated system can be introduced in polyclinics and hospitals to clinically support the clinicians to confirm their manual diagnosis of foot screening.

Keywords: diabetic foot, neuropathy, vascular, infrared thermography, thermogram, DD-DT-CWT, LSDA.

1. INTRODUCTION

Diabetes is a chronic major endocrine disorder caused by deficiency in the production of insulin, or inefficacy in the usage of insulin (1). Such an inadequacy may raise the ~~blood~~ glucose concentration levels in the blood, potentially ~~which may cause severe damages~~ damaging ~~to~~ the blood vessels and nerves (1). In 2014, approximately 422 million adults globally were living with diabetes and the diabetes global prevalence has almost doubled since 1980, from 4.7% to 8.5% (2).

Progressively, diabetes can damage the various parts of the body. The most common problem of diabetes is diabetic foot disease (DFD). The pathologies of DFD are primarily peripheral arterial disease and peripheral neuropathy which may lead to foot ulceration (3). The lifetime risk of a diabetic patient ~~to~~ in developing a foot ulcer is about 15-25% (4). Moreover, it is approximated that 45-

60% of the diabetic patients with foot ulcers are ~~because of~~attributed to neuropathy, whereas about 45% of them may be due to the ~~-~~combination of both ischemic and neuropathic conditions (5-8). The foot ulceration may further result in amputation particularly when osteomyelitis or wound infection is present. In fact, almost 85% of the amputations are due to infectious and non-healing foot ulcerations (9).

Human beings are regarded as homeotherms with the capability to sustain inner body temperature despite variations in the surrounding temperature by altering heat loss and heat production rates (10-12). Nonetheless, this thermoregulatory mechanism of the human body may still be altered by pathologies especially autonomic neuropathy, peripheral arterial disease and inflammations (13). In the case of DFD, peripheral arterial disease and neurological disorders can change the temperature of the lower limb (14). The studies have reported that temperature variations in the plantar foot areas are ~~be~~ due to the diabetic foot complications (15-21). Clinically, temperature gradient on the lower limbs is often assessed by gently running the back of the hand from below the knee distally to the toes~~The general clinical practice of temperature examination is the manually palpating of the foot~~ (13). ~~Nevertheless~~Evidently, this method is ~~less decisive to determine~~not sensitive to the subtle temperature changes in ~~the~~ different parts of the plantar foot ~~plantar~~.

The infrared thermography (IRT) is a fast, non-invasive and non-contact method which allows the visualization of plantar temperature distribution. The IRT radiations are harmless, but captures the body heat profile (22). Hence, the applications of IRT have significantly increased over the years especially to study the ~~diabetes~~ diabetic foot related complications (23). It is used to observe morphology of the skin temperature pattern caused by blood perfusion. In conditions where blood circulation at the peripheral limbs are reduced (ischemic),

there will be a change in the temperature patterns (23). In general, an ischemic foot ~~will~~ tends to appear cold and ~~warm for~~conversely a neuropathic foot is often warm (24).

In recent years, several authors have studied the plantar foot temperature variations in diabetic patients using IRT (25). As listed in Table 1-4, the *four* types of analysis namely "separate lower limb temperature", "asymmetric temperature", "temperature distribution", and~~,~~ "independent thermal and physical stress" ~~analysis~~ are proposed to study the ~~diabetes~~ diabetic foot. The separate lower limb temperature analysis (26-33) provides only temperature ranges for various study groups and cannot localize the risk regions. In asymmetric temperature analysis (34-47), plantar temperature is compared between both (left and right) foot. This analysis is unable to identify the risk regions if the same complications exist in both foot and also, partial or whole foot amputation have to be excluded due to the absence of the ~~foot~~ plantar foot region to be compared. In temperature distribution analysis (48-53) each foot is analyzed independently. However, the irregular plantar thermal patterns in diabetes patients make the classification difficult. In independent thermal and physical stress analysis (54-61) the plantar temperature reaction with respect to the applied external stimulus are independently evaluated and analyzed. The external stress that consists of walking or immersing the limb into cold or hot water ~~for a period~~momentarily may result in subjects feeling uncomfortable and inconvenient. Hence, there is a need to have consistent accurate algorithm which can effectively detect and analyze the minute thermal variations in the diabetic foot.

This study aims to automatically detect the diabetic foot (with and without neuropathy) using plantar foot thermogram. The diverse thermal variations of the plantar foot are quantitatively analysed and characterised. First, the plantar foot

thermograms are segmented and then warped. The warped grayscale images are decomposed using double density-dual tree-complex wavelet transform (DD-DT-CWT). Then various texture and entropy features are extracted from these decomposed coefficients. The separately extracted features of left, right and both foot is subjected to various data reduction techniques and ranked based on *F*-value. Finally, the ranked features are fed to the various classifiers to evaluate the highest performing classifier. The block diagram of the proposed system is presented in Figure 1.[IIA2]

Table 1: Separate lower limb temperature analysis.

Reference (Year)	**Methodology**	**Findings**
Ammer et al, 2001. (26)	• Physical examination of feet • Neurological assessment • Thermal imaging • Single Measure Intraclass Correlation • Mann-Whitney U-test	• No relationship between skin changes and increased skin temperature
Melnizky et al, 2002. (27)	• Physical examination of feet • Nerve conduction test • Thermal imaging • SPSS 10.0 for statistical analysis	• A pathological temperature gradient was detected on the right limb of 36 diabetes patients (mean pathological gradient: -0.27±0.68*K* vs -1.84±0.81*K*) whereas 39 patients on the left limb (-0.77±1.15*K* vs -1.49±1.21*K*) • No correlation between temperature measurements and nerve conduction
Sun et al, 2005. (28)	• Electromyography for sympathetic skin response (SSR) test • Thermal imaging • Compute average temperature of six sub regions on each healthy sole • Analyze sole temperature normalization relative to forehead temperature of diabetes patients • SPSS for statistical analysis	• Highest temperature (29.3±0.9^{o}*C*) in the arc areas and lowest for the toes (26.2±1.2^{o}*C*). • Diabetes patients without sympathetic skin response (SSR) had higher mean plantar temperature (27.6±1.8^{o}*C*) compared to those with SSR (26.8±2.2^{o}*C*) • Equilibrium temperature is achieved at mean plantar temperature (27.8±1.0^{o}*C*) after 15 *minutes*

Sun et al, 2006. (29)	• Seattle Wound Classification system • Thermal imaging • Electromyography for sympathetic skin response (SSR) test • Neurological assessment • SPSS for statistical analysis	• At risk diabetes patients with pre-ulcerative skin and without SSR had highest mean foot temperature (30.2±1.3^{o}C) compared to diabetes patients without SSR (27.9±1.7^{o}C), diabetes patients with SSR (27.1±2.0^{o}C), and normal subjects (26.8±1.8^{o}C)
Sun et al, 2008. (30)	• Seattle Wound Classification system • Thermal imaging • Electromyography for sympathetic skin response (SSR) test • Neurological assessment • Nerve conduction test • SPSS for statistical analysis	• At-risk class is 13.4 times more likely to develop plantar ulcerations than the diabetes patients with and without SSR during the 4-year period
Nishide et al, 2009. (31)	• Ankle Brachial Index (ABI) • Toe Brachial Index (TBI) • Achilles tendon reflex and vibratory perception • Semmes-Weinstein monofilament test • Thermography • Ultrasonography • Fisher's exact probability test • Mann-Whitney U-test • SPSS for statistical analysis	• Ultrasonography and thermography detect inflammation symptoms in 10% of the calli in diabetes class whereas no inflammation detected in the normal class.
Bharara et al, 2010. (32)	• Thermal imaging • Thermal index • Image J Software	• Thermal index/ wound inflammatory index moved from negative to positive ($p<0.05$) prior to reaching zero
Bagavathiappan et al, 2010. (33)	• Anthropometric measurements • Glycated hemoglobin (HbA1c) • Neuropathy assessment • Vascular sufficiency assessment • Thermal imaging • SPSS for statistical analysis	• Diabetes neuropathy patients recorded highest foot temperature (32 – 35^{o}C) than non-neuropathy diabetes patients (27 – 30^{o}C) • Higher mean foot temperature (MFT) for Diabetes neuropathy patients • No relationship between MFT and glycated hemoglobin

Table 2: Asymmetric temperature analysis.

Reference (Year)	**Methodology**	**Findings**

Harding et al, 1998. (34)	• Infrared imaging • Radiography	• Out of the 26 diabetes patients with positive thermograms, 21 of whom are confirmed with osteomyelitis by radiological evidence • Positive thermogram is described as at least 0.5^{o}C rise in temperature of the affected foot skin with respect to the contralateral foot sole
Kaabouch et al, 2009a. (35)	• Infrared imaging • Segmentation • Geometric transformation • Asymmetry analysis	• Able to detect and determine inflammation and ulcers accurately and rapidly
Kaabouch et al, 2009b. (36)	• Infrared imaging • Automatic thresholding • Geometric transformation • Asymmetry analysis • Features extraction	• Genetic algorithm yields superior thresholding results • Low and high order statistics effectively enhance the asymmetry analysis in detecting foot abnormalities
Kaabouch et al, 2010. (37)	• Infrared imaging • Segmentation • Geometric transformation • Asymmetry analysis	• Genetic algorithm produces superior thresholding results
Kaabouch et al, 2011a. (38)	• Infrared imaging • Segmentation • Geometric transformation • Asymmetry analysis and abnormality identification • Features extraction	• Genetic algorithm produces superior thresholding results • Low and high order statistics effectively enhance the asymmetry analysis in detecting foot abnormalities
Kaabouch et al, 2011b. (39)	• Infrared imaging • Genetic algorithms • Asymmetry analysis-based scalable scanning	• Genetic algorithms effectively crop the feet from background and eliminate most noise • Scalable scanning method yield fewer false abnormal regions
Liu et al, 2013. (40)	• Infrared imaging • Foot segmentation • Feet registration • Abnormal detection	• Active contours without edges method acquire reasonable result • Automated detection of pre-symptoms ulceration by computing temperature difference of the feet • 2.2^{o}C as the clinical relevant difference
Peregrina-Barreto et al, 2013. (41)	• Infrared imaging • Color characterization • Foot angiosomes and color classification	• The temperature estimate difference between corresponding angiosomes can be used to screen for abnormality
van Netten et al, 2013. (42)	• Infrared imaging • Mean temperature of whole foot and regions of interest	• Mean temperature of contralateral and ipsilateral foot is the same in patients with localized problems • Temperature at ROI was more than 2^{o}C compared to the similar area in contralateral foot and to the mean of the entire ipsilateral foot

		• Mean temperature differences between the contralateral and ipsilateral foot was more than 3^{o}C in patients with diffuse problems
Peregrina-Barreto et al, 2014. (43)	• Infrared imaging • Color characterization • Temperature estimated difference • Hot spots detection	• HSE capable of detecting abnormal small areas in the early phase that were not detected by ETD estimator
van Netten et al, 2014. (44)	• Infrared imaging • Clinical foot assessments • Kruskal-Wallis test • Receiver operating characteristic (ROC) curve and area using SPSS	• Optimal cut-off value for skin temperature in identifying diabetes foot problems was difference of 2.2^{o}C between contralateral spots, with 76% sensitivity and 40% specificity • Optimal cut-off values for skin temperature to decide the urgency for treatment was difference of 3.5^{o}C between left and right foot mean temperature, with 89% sensitivity and 78% specificity
Vilcahuaman et al, 2014. (45)	• Infrared imaging • Image processing	• In the clinical study, 10% of the diabetes patients had signs of significant hyperthermia on the foot plantar with temperature difference of more than 2.2^{o}C
Vilcahuaman et al, 2015. (46)	• Infrared imaging • Image processing	• High risk group had significantly higher temperature (32±2^{o}C) than medium risk group (31±2^{o}C) • In the study, 9 out of 82 diabetes patients had significant hyperthermia
Liu et al, 2015. (47)	• Infrared imaging • Foot segmentation • Registration optimization • Asymmetric analysis	• The study yielded an accuracy of 95% with 35 out of the 37 diabetic foot ulcers identified • All three Charcot feet are successfully detected.

Table 3: Temperature distribution analysis.

Reference (Year)	**Methodology**	**Findings**
Branemark et al, 1967. (48)	• Infrared imaging • Clinical assessment	• Abnormal emission patterns from hand and feet of all diabetes patients • Reduced emission on the metatarsal and toes areas
Nagase et al, 2011. (49)	• Infrared imaging • Conceptual classification comprising of 20 categories of	**Normal** • 48 feet (or 75%) are characterized to the seven categories and the

		plantar thermography patterns	remaining 16 feet characterized as atypical • The Id category (butterfly pattern) is mostly identified with 30 feet (or 46.9%) **Diabetes** • 225 (or 87.2%) diabetes feet are characterized to 18 categories and the remaining 33 feet (or 12.8%) as atypical • The IIa category (medial and lateral plantar arteries undamaged) is mostly identified with 101 feet (or 39.1%)
Oe et al, 2013. (50)	• MRI scans • Infrared imaging • Ankle-brachial index (ABI) • Toe-brachial index (TBI) • Nerve conduction velocity • SPSS for statistical analysis		• Ankle pattern is mostly common in patients with osteomyelitis • Sensitivity = 60% • Specificity = 100% • PPV = 100% • NPV = 71.4%
Mori et al, 2013. (62)	• Ankle-brachial index (ABI) • Toe-brachial index (TBI) • Achilles tendon reflex • Semmes-Weinstein monofilament test • Vibratory sensation test • Infrared imaging • Image partitioning algorithm • T test or chi square test		**Normal** • 47 feet are characterized to the four categories and the remaining 17 feet characterized as anomalous • The type 1 (butterfly pattern) (44%) is mostly identified **Diabetes** • 198 diabetes feet are characterized to six categories and the remaining 60 feet as atypical • The type 2 (46%) is mostly identified
Bharara et al, 2014. (51)	• Clinical assessment • Semmes Weinstein monofilament • Vibratory perception threshold • Infrared imaging		**Normal** • Subjects are mostly represented by Id category (Butterfly Pattern) during measurements with 47.2% at rest, 13.8% at post stress and 27.8% at recovery **Diabetes** • Subjects are mostly represented by IIa category (medial and lateral plantar arteries undamaged) during measurements with 50% at rest, 50% at post stress and 28.57% at recovery
Hernandez-Contreras et al, 2015a. (52)	• Infrared imaging • Grayscale characterization		**Normal**

	• Arch segmentation based on histogram distribution • Mathematical morphology	• Butterfly pattern is presented in the subjects and pattern spectrum is same as oval • Mean percentage of pixels for control group is highest in quadrant 4 with 88.05% **Diabetes** • Pattern spectrum is irregular due to the dissimilar pattern • Mean percentage of pixels is 28.87% for diabetes group in quadrant 3.
Hernandez-Contreras et al, 2015b. (53)	• Infrared imaging • Grayscale characterization • Foot segmentation • Temperature pattern • Mathematical morphology • Pattern spectrum • Multilayer perceptron • K-fold cross validation	• Proposed technique achieved average classification rate of 94.33%

Table 4: Independent thermal and physical stress analysis.

Reference (Year)	**Methodology**	**Findings**
Fushimi et al, 1996. (54)	• ECG • Ankle pressure index • Infrared imaging • Ultrasonic imaging	**Normal** • All subjects had normal pattern **Diabetes** • 43 had normal, 19 increasing and 26 decreasing and 24 flat patterns
Fujiwara et al, 2000. (55)	• Infrared imaging • Ankle-brachial index • Doppler meter • Motor nerve conduction velocity • Sensory nerve conduction velocity • ECG • Schellong's test • Photo-dispersion method • ANOVA with Neuman-Keuls multiple comparison test	• Smaller skin temperature drops in diabetes patients compared to normal subjects after immersing into cold water • Diabetes patients had lower skin temperature recovery rate due to causal factors such as peripheral arterial sclerosis, abnormal blood coagulation fibrinolysis and sympathetic nerve dysfunction
Hosaki et al, 2002. (56)	• Infrared imaging • Laser Doppler blood flowmeter • Hot loading at 36 ^{o}C • Cold loading at 20 ^{o}C • Compute recovery ratio	• Recovery ratios for the 27 diabetes patients were in the range of 0-93.5% and the average was 34% • Blood flow and recovery ratio were correlated ($r = 0.634$, $p<0.0001$) • Ratio of blood flow after cold loading over the blood flow after

		hot loading was in the range of 38.1% - 122% and average of 80.6%. • This ratio and recovery ratio is correlated (r = 0.502, p<0.0001)
Balbinot et al, 2012. (57)	• Clinical assessments • Heart rate variability • Infrared imaging • Electromyography • Statistical analysis	**Diabetes** • Interdigital anisothermal method performed better than thermal recovery index with 46.2% specificity and 81.3% sensitivity **Prediabetes** • All three tests achieved 25% specificity and 80% sensitivity equally
Barriga et al, 2012. (58)	• Infrared imaging • Motion tracking of thermal features • Exponential curve fitting	• Diabetes neuropathy patient recorded recovery rate of 2% at the two toes and approximately 0.4% at the heel • Normal subject recorded high recovery of 4% at the medial arch as compared to less than 1.5% in the diabetes neuropathy patient
Najafi et al, 2012. (59)	• Two pre-defined paths of 50 and 150 steps • Infrared imaging • Image processing • Student t test • ANOVA	• In Charcot neuroarthropathy group, the decreased in temperature for non-affected foot is 1.9 folds more than the affected foot • Plantar temperature for both foot in Charcot neuroarthropathy group significantly increased beyond 50 steps and remain higher on the affected foot at 200 steps
Balbinot et al, 2013. (60)	• Clinical assessments • Infrared imaging • Data analysis • Statistical analysis	• Significant difference in the average temperatures of normal subjects between the two days before and after cold stress test compared to no difference in the average temperatures for diabetes patients • Rewarming index of both groups did not differ between the two days
Yavuz et al, 2014. (61)	• Walking on pressure shear plate • Treadmill walking • Infrared imaging • Peak shear stress and peak resultant stress • Statistical analysis	• Significant correlation between temperature rises and peak shear stress (r =0.78) • Increased in plantar temperature can predict the site of peak resultant stress and peak shear stress in 39% and 23% of the subjects
Agurto et al, 2015. (63)	• Cold stimulus • Infrared imaging • Independent component analysis (ICA)	• Components 2, 6 and 8 significantly differentiate the normal and diabetes peripheral neuropathy patients • Higher recovery rate in normal subjects for component 6

	• Diabetes peripheral neuropathy patients have lower temperature recovery rate in most parts of the foot plantar

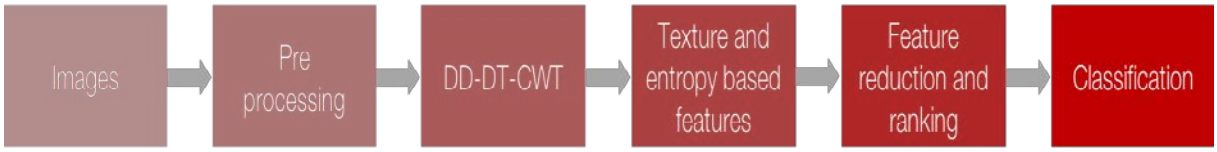

Figure 1: Block diagram of the proposed system for the detection of diabetic foot (with and without neuropathy).

2. MATERIALS & METHODOLOGY

Study Population

In this study, ~~normal~~ healthy adults and ~~diabetes~~ diabetic patients with and without neuropathy classes were considered. A total of 51 healthy subjects and 66 diabetic patients (33 non-neuropathic and 33 neuropathic) were recruited from Ngee Ann Polytechnic and Singapore General Hospital (SGH), Diabetes & Metabolism Centre (DMC) respectively ~~under similar conditions~~. Except for healthy and ~~diabetes~~ diabetic non-neuropathic groups, several patients in the ~~diabetes~~ diabetic neuropathic group had toes amputation. The diabetic foot thermogram data collection was approved by SingHealth Centralised Institutional Review Board (CIRB) **(CIRB Ref: 2016/3044).** The normal foot thermograms data collection was approved by Ngee Ann Polytechnic-Institutional Review Board (NP-IRB) **(NPIRB-P0175-2017-ECE-AMA6)**. The demographic information of normal and ~~diabetes~~ diabetic (with and without neuropathy) groups are shown in Table 5[IIA3]. The participants were briefed about the study before signing the patient consent form.

Table 5: Demographic information of normal and ~~diabetes~~ diabetic (with and without neuropathy) groups (mean±standard deviation).

	Normal group	~~Diabetes~~ Diabetic group	
		Non-neuropathy	Neuropathy
Total	51	33	33
Female	27	15	9
Male	24	18	24
Average Age (*years*)	48.41±11.12	56.18±14.71	62.33±10.63
Average Body Mass Index (BMI) (kg/m^2)	23.73±3.32	25.08±5.31	27.84±4.37

Thermogram acquisition

The plantar foot thermograms were acquired in a controlled room with temperature = 20±1^{o}C and humidity = 55±5%. The subjects were required to remove their foot wear~~s~~, socks, and clean their feet. The subjects then remained seated ~~in a supine position~~ on the treatment bench for 15 minutes. The purpose is to reach the thermal equilibrium before capturing the thermogram. The plantar foot thermograms were captured using **Thermographic System VarioCAM© hr head 680/30 *mm*** positioned at a focus distance of 1 *meter* from the feet. The acquired plantar foot thermograms are converted into grayscale images as shown in Figure 2(a)-(c) with temperature scale ranging from 20 to 34℃. The infrared camera automatically calibrates the temperature scale based on the coldest and hottest points in the scene. The thermograms are kept in ***irbis*** format after acquisition and thereafter converted into ***bmp*** format for the following image analysis.

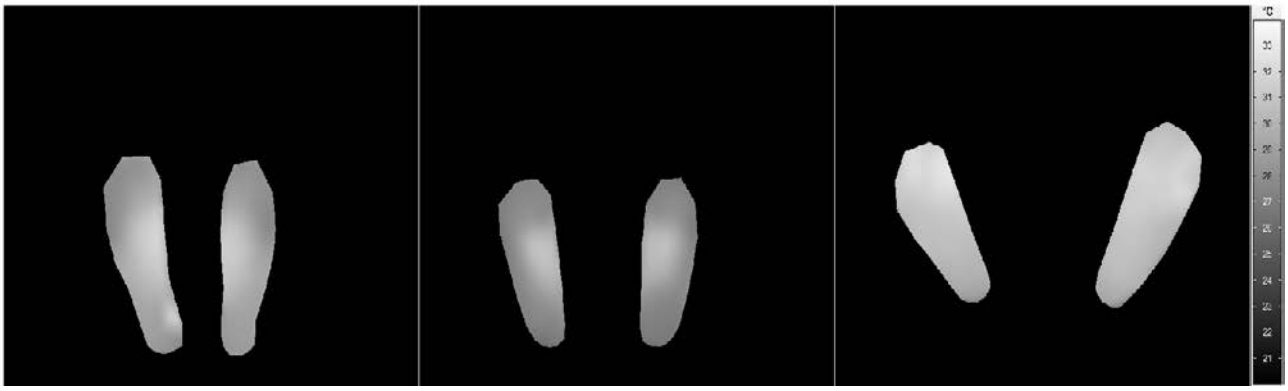

(a) (b) (c)

Figure 2(a) – (c): Grayscale images of plantar foot thermograms (°C): (a) normal, ~~diabetes~~ diabetic (b) without neuropathy and (c) with neuropathy.

Methodology

In this study, the grayscale plantar foot thermograms are segmented without five toes and warped into standard size and shape (64). This ensures uniform plantar foot region for analysis ~~of~~ among the three groups. Subsequently, the temperature data within the region of interest (ROI) is decomposed using double density-dual tree-complex wavelet transform (DD-DT-CWT), which is able to localise features in various orientations (65). Various feature values (entropy and texture based) are extracted from the decomposed images of left, right and both (left and right) foot. These large number of features are reduced and ranked prior to the classification.

Plantar foot segmentation

The plantar foot region is manually delineated using a polygon of 16 points. These points are placed on the boundary of the foot and are joined by straight lines that enclosed the plantar foot excluding the toes. The segmented left foot is then flipped in the same orientation as right foot for equal comparison prior to the subsequent analysis. The marking and delineation of the region of interest (ROI) is depicted in Figure 3(a)-(b).

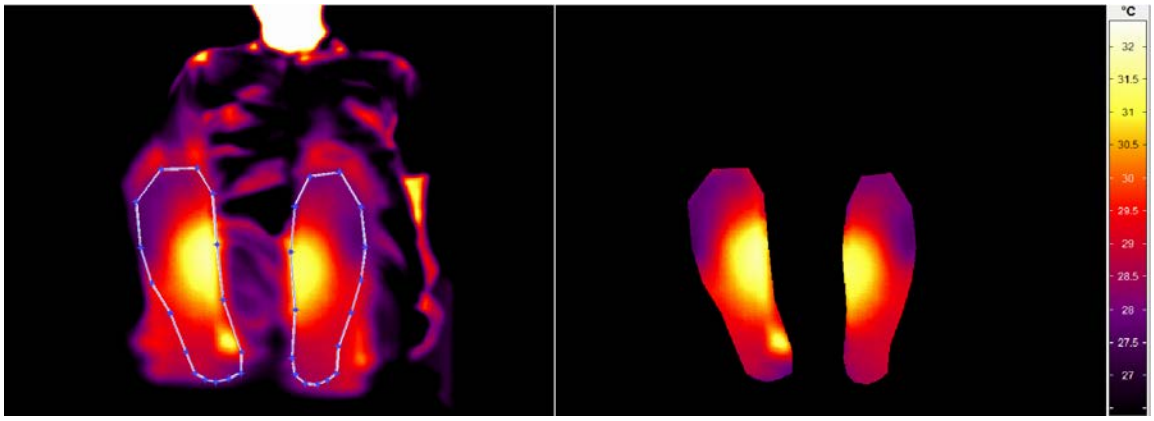

(a) (b)

Figure 3(a) – (b): Plantar foot segmentation: (a) marking and (b) delineation of region of interest (ROI) using polygon.

Double density-dual tree-complex wavelet transform (DD-DT-CWT)

The double density-dual tree-complex wavelet transform (DD-DT-CWT) structure as seen in Figure 4 is simultaneously derived through *four* different wavelets and *two* different scaling functions (66), in which two wavelets and one scaling are used for imaginary and real components of a complex wavelet respectively. There are two filter banks in this complex transformation, namely *primary* and *dual* filter banks (67). The analysis (decomposition) low pass [high pass] filters of *primary* and *dual* filter banks are represented as $H_0(z)$ $[H_1(z),\ H_2(z)]$ and $\widetilde{H_0(z)}$ $[\widetilde{H_1(z)},\ \widetilde{H_2(z)}]$ respectively. The respective wavelet and scaling functions of *primary* filter bank are defined as (66):

$$\psi_{h_i}(t) = 2\sum_M h_i[M]\phi_h(2t - M) \ \ for\ i = 1, 2 \tag{1}$$

$$\phi_h(t) = 2\sum_M h_0[M]\phi_h(2t - M) \tag{2}$$

where the impulse response of $\boldsymbol{H_0(z)}$ and $\boldsymbol{H_i(z)}$ are $\boldsymbol{h_0[M]}$ and $\boldsymbol{h_i[M]}$ respectively, and $\boldsymbol{z}$ is the z-transform where $\boldsymbol{z = e^{j\omega}}$. The wavelet and scaling functions for both the *primary* and *dual* filter banks are identically defined. In general, the *primary*

and *dual* filter banks are designed in such a way that the sub-bands of upper and lower filter banks are interpreted as the real and imaginary part of the transformation. Specifically, the wavelets of the real part have to be the Hilbert transform of the wavelets associated to the imaginary part. The 2 dimensional (2D) oriented higher density complex transformation of DD-DT-CWT has more directional selective wavelets that are widely applicable for pattern recognition and image processing (66). In this study, DD-DT-CWT decomposes the pre-processed images and yielded 32 directional wavelet sub-bands. The 32 directional wavelet ~~sub~~ sub-bands of DD-DT-CWT for normal, and ~~diabetes~~ diabetic without and with neuropathy foot thermogram are shown in Figure 5(a)-(c).

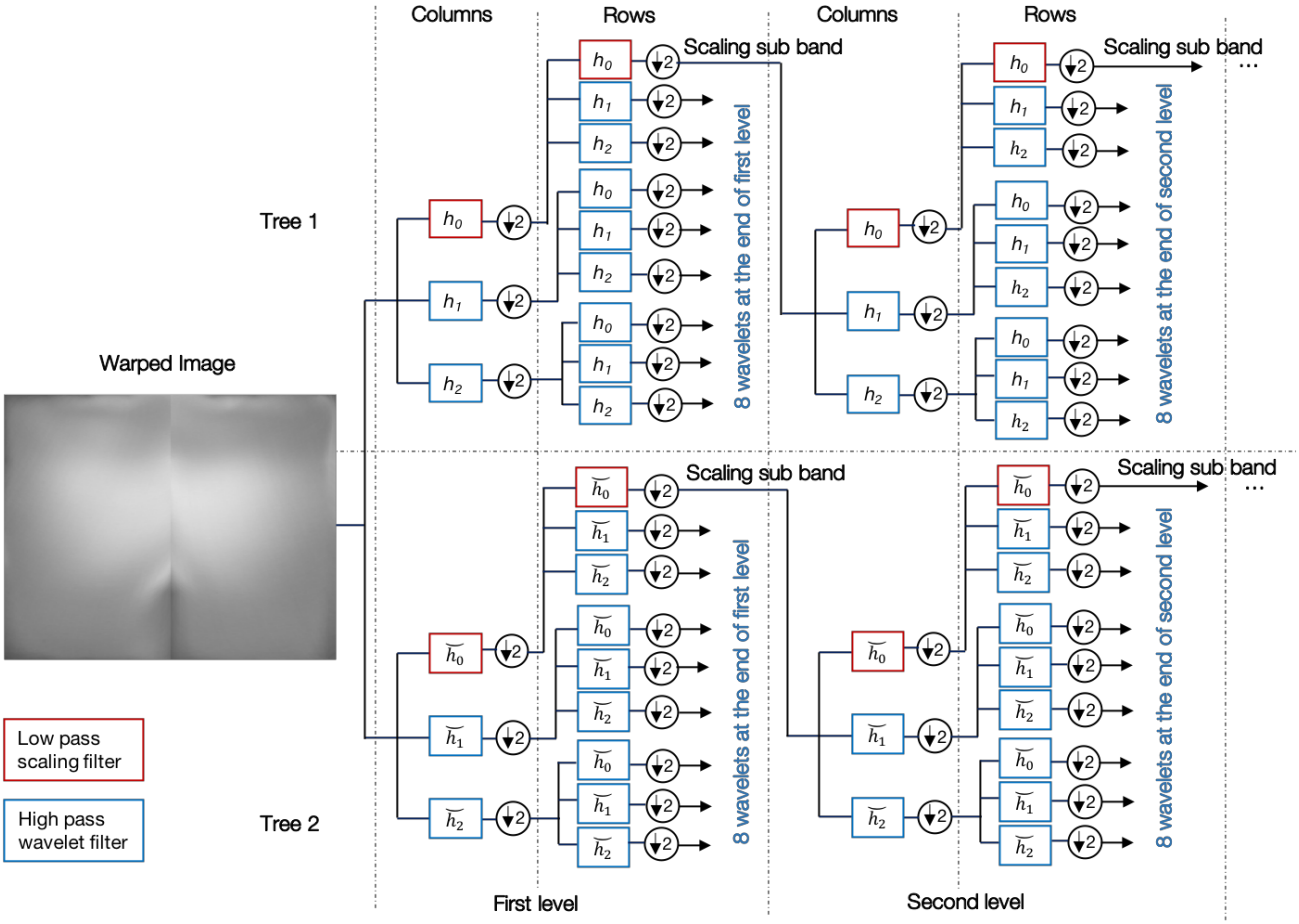

Figure 4: Typical structure of DD-DT-CWT of two level.

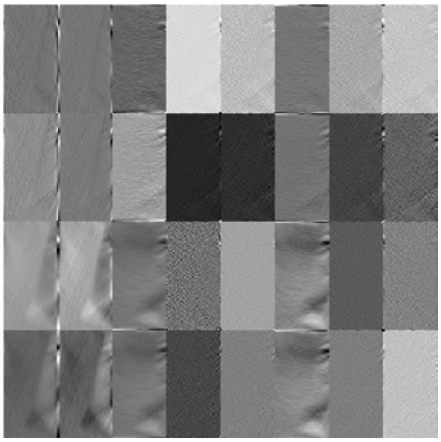

(a)

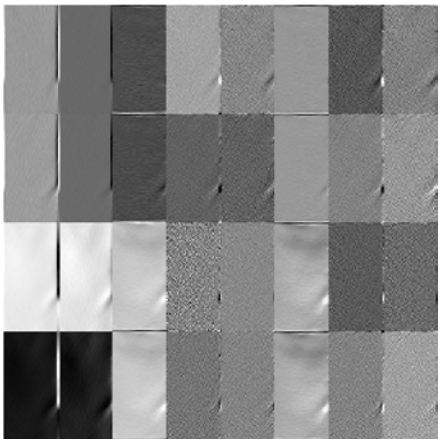

(b)

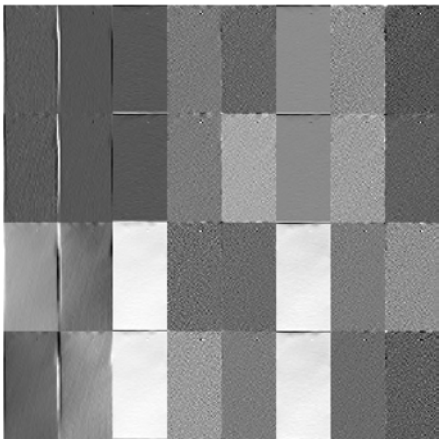

(c)

Figure 5(a)-(c): 32 directional wavelet ~~sub~~ sub-bands of DD-DT-CWT for (a) normal, and ~~diabetes~~ diabetic (b) without and (c) with neuropathy foot thermogram.

Feature extraction

In this study, the entropy and texture-based features are extracted from the decomposed DD-DT-CWT images. We have extracted Hu's invariant moment (68), gray level co-occurrence matrix (GLCM) (69) and entropies (70-77) features from the decomposed left, right and both (left and right) foot images.

Feature reduction

In this work, we have obtained 4032, 4032 and 8064 features for left, right and both foot studies respectively. It is tedious, and computationally intensive to analyse such huge number of features. Hence, we have used dimensionality reduction techniques allowing the original data to be represented in a subspace (78). In this study, *five* dimensionality reduction techniques namely neighbourhood preserving embedding (NPE) (79, 80), locality preserving projection (LPP) (81), locality sensitivity discriminant analysis (LSDA) (82), principal component analysis (PCA) (83) and kernel PCA (KPCA) (84) were used to choose the best performing method.

Feature selection

The feature selection strategies are used to remove the redundant and irrelevant information (85). This helps to boost the classifier performance, computational time and cost (78). In this study, One-way? Analysis of Variance (ANOVA) statistical method was implemented to determine and rank the distinct features based on *P*-value and *F*-value respectively (86). The lower *P*-value < 0.0001 and high *F*-value denotes highly discriminatory features among the *three* classes. Thereafter, the ranked features are individually input into the classifiers.

Classification

The classifiers are used to automatically classify the unknown (test) data (87). In this study, the extracted features are ranked and fed one by one to the various classifiers to choose the least number of features needed for classification. Our classifiers are trained and tested using 10-fold cross validation method (88). The classifiers used in this work are decision tree (DT) (89), *k* nearest neighbor (*k*NN) (90), linear discriminant analysis (LDA) and quadratic discriminant analysis (QDA) (91, 92), probabilistic neural network (PNN)[IIA4] (93), and support vector machine (SVM) (94).

3. RESULTS

The segmented grayscale plantar foot (without toes) images are warped into a standard image size of 280 x 140 pixels. For each foot, a mixture of 4032 entropy and texture-based features are extracted. The actual dimension of the extracted feature is then reduced to *thirty* using LSDA and subsequently ranked using *F*-value with ANOVA. The significantly ranked features extracted from the left, right and both foot are tabulated in Appendix A (Table 9-11).

The ranked features of left, right and both (left and right) foot are then fed to the classifiers one by one to determine maximum classification performance with minimum number of features. The classification performance using various feature reduction techniques are presented in Table 6-8. It can be observed that LSDA coupled with classifiers yielded the highest classification performance for left, right and both foot. In Table 6, LSDA coupled with ~~SVM-~~SVM-RBF classifier achieved 93.16% accuracy, 93.94% sensitivity and 94.12% specificity using *eight* left foot features. Meanwhile, LSDA coupled with ~~SVM-~~SVM-RBF classifier in Table 7 attained 91.45% accuracy, 90.91% sensitivity and 98.04% specificity using

eight right foot features. Lastly, in Table 8, LSDA coupled with *k*NN classifier obtained 93.16% accuracy, 90.91% sensitivity and 98.04% specificity using *four* combinations of both foot features.

Table 6: Results of classification using left foot features with various reduction methods.

Reduction method	**Classifier**	**No. of Features**	**Acc (%)**	**Sen (%)**	**Spec (%)**
kpcaLinear	PNN	2	62.39	77.27	80.39
kpcaPolynomial	*k*NN	3	57.26	75.76	72.55
kpcaPolyPlus	*k*NN	3	57.26	75.76	72.55
Lpp	SVM RBF	3	59.83	78.79	64.71
Lsda	SVM RBF	8	93.16	93.94	94.12
Npe	SVM RBF	5	62.39	86.36	78.43
Pca	PNN	3	64.10	80.30	80.39

Table 7: Results of classification using right foot features with various reduction methods.

Reduction method	**Classifier**	**No. of Features**	**Acc (%)**	**Sen (%)**	**Spec (%)**
kpcaGaussian	PNN	2	47.01	30.30	88.24
kpcaLinear	LDA	2	58.97	69.70	80.39
kpcaPolynomial	PNN	3	59.83	74.24	68.63
kpcaPolyPlus	PNN	3	59.83	74.24	68.63
lpp	*k*NN	4	57.26	60.61	74.51
lsda	SVM RBF	8	91.45	90.91	98.04
npe	QDA	3	58.12	69.70	70.59
pca	LDA	3	59.83	71.21	76.47

Table 8: Results of classification using both (left and right) foot features with various reduction methods.

Reduction method	Classifier	No. of Features	Acc (%)	Sen (%)	Spec (%)
kpcaGaussian	Decision Tree	2	48.72	66.67	52.94
kpcaLinear	SVM RBF	3	55.56	71.21	72.55
kpcaPolynomial	SVM RBF	6	58.12	81.82	72.55
kpcaPolyPlus	SVM RBF	6	58.12	81.82	72.55
lpp	LDA	3	58.12	84.85	62.75
lsda	*k*NN	4	93.16	90.91	98.04
npe	*k*NN	4	63.25	66.67	80.39
pca	SVM RBF	3	55.56	71.21	72.55

4. DISCUSSION

IRT has been effective in detecting diabetic foot related complications based on feet temperature distribution (25). Adam et al. (95) recently developed a *two-class* automated detection system (normal and ~~diabetes~~ diabetic without neuropathy) based on IR images of ~~foot~~ feet using discrete wavelet transform (DWT) and higher order spectra (HOS) coefficients. Their proposed system yielded highest classification accuracy of 89.39%, sensitivity of 81.81% and specificity of 96.97% using only *five* nonlinear features. Our present study is *three-class* diabetic foot detection system (normal, ~~diabetes~~ diabetic with and without neuropathy) using left, right and both (left and right) foot features extracted from thermograms. The developed system yielded best classification performance of 93.16% accuracy, 90.91% sensitivity and 98.04% specificity using only *four* distinct foot features extracted from both foot. To the best of our knowledge this is the first automated system to classify the normal, ~~diabetes~~ diabetic with and without neuropathy using thermograms of foot.

The various methods used for thermogram analysis are summarised in Table 1-4. Bharara et al. (32) presented a quantitative thermography method ~~using~~ through thermal index for diabetic foot ulcer assessment using a single case and correlated it with the standard wound measurement method. The thermal index/wound inflammatory index moved from negative to positive ($p<0.05$) prior to reaching zero. Nevertheless, the index analysis requires more patients. Liu et al. (47) proposed a technique involving asymmetric analysis together with colour images segmentation and, non-rigid landmark based registration B-splines of right and left feet. Their method is able to determine diabetic foot ulcers with 95% accuracy (35 out 37), which included all the Charcot foots. Hernandez-Contreras et al. (53) proposed characterization technique to distinguish the thermal patterns of normal and ~~diabetes~~ diabetic patients. Their technique obtained an average classification rate of 94.33% using the extracted features. Balbinot et al. (60) compared the plantar temperatures and analysed the plantar re-warming index repeatability after cold stress on two separate days for ~~diabetes~~ diabetic and normal groups. ~~The proposed study observed that the~~The rewarming index presented good repeatability after cold stress between two days a week apart in both groups. However, the sample size ~~is~~ was small ~~because this is a pilot study~~ and the ~~clinical assessment performed~~study did not identify ~~the diabetes~~ diabetic patients with neuropathy.

The majority of these studies presented in Table 1-4 did not implement feature extraction and classification techniques. Indeed, it may not be simple to capture the minute abnormal temperature variations by just visually examining the feet thermogram (87). Therefore, this study has adopted image analysis techniques for diabetic foot detection system of *three* classes using DD-DT-CWT. The DD-DT-CWT is a dominant multi-resolution analysis technique whereby the number (density) of high frequency (detail) sub-bands increases with increasing transformation (66). This allows the DD-DT-CWT coefficients to better capture

subtle sudden variations within the pixels, which are mostly present in the high frequency components of the images (96). Besides, the features can be localised in many directions due to the main properties of DD-DT-CWT, such as double density wavelets, shift invariance and directional selectivity (65). This is essential in ~~an~~ image analysis as it provides significant and distinct information relating to the ~~diabetes~~ diabetic foot classes (with and without neuropathy).

Equally important, ~~diabetes~~ diabetic foot (with and without neuropathy) features extracted during real clinical circumstance may overlap and ~~also~~ possibly redundant. Hence, there is a need to efficiently differentiate these features into its respective classes. Several dimension reduction-based methods are performed in this study ~~that lead~~ to ~~acquiring~~ achieve distinct~~ively reduce~~ features. In comparison to other ~~projection~~ methods, LSDA reduced features of left, right and bilateral foot yielded highest classification performances as seen in Table 6-8. The intra class margin of LSDA effectively characterise the separation of various classes without needing prior data distribution information (78). Equally important, the significant LSDA reduced features are determined based on the *F*-value ranked in descending order as listed in Appendix A (Table 9-11). The *three* classes showed good discriminatory characteristics for all feature types (left, right and bilateral foot) based on the mean and standard deviation values. Therefore, this allows the developed system to yield maximum classification results.

The association between diabetic foot and heat pattern on the plantar foot is subtle and often nonlinear (87). Therefore, the development of computer aided system (CAD) is essential in helping to interpret the plantar thermograms. The knowledge discovery and data mining algorithms may provide improvement to the thermogram based CAD system in various main areas. First, screening clinicians may experience possible visual overloading. With thermogram based CAD system, ~~diagnosis~~ diabetic foot classification workload can be reduced, and

more attention can be given on complicated cases. ~~Thus,~~This may ~~enhancing~~ enhance the medical care rendered to difficult cases. Secondly is the inter observer variability. Thermogram diagnosis based on human can be subjective and the qualities may vary extensively. Thus, objective technique based on mathematics and computer science can help in objectifying the ~~diagnosis~~ classification and decrease the inter-observer variability. Finally, the quality of diagnosis. To a large extent, the progress of thermogram diagnosis based on human depends on training level and experience of the screening clinicians. Meanwhile, the progress of CAD system is based on the software and hardware in which computing machinery is increasingly becoming more potent. Moreover, the software domain progresses by integrating and from developing better image processing algorithms. Hence, CAD system may be able to outperform the clinicians based on cost, accuracy and speed.

The following are the advantages of our developed system:

1. Yielded maximum classification accuracy of 93.16% in classifying *three* classes (normal, ~~diabetes~~ diabetic with and without neuropathy).
2. Developed system is fast and computationally less intensive.
3. Proposed model is noncontact, robust and fully automated.
4. Needs only *four* foot (left and right) features to yield maximum classification performance.

The drawbacks of the developed system are as follows:

1. Used only 117 participants (51 healthy individuals and 66 diabetic patients).
2. The developed system is semi-automated.
3. The IRT camera is expensive.
4. The results are yet to be validated on prospective diabetic patients.

In future, we are planning to continue this work using more subjects in each class to make the system more robust and accurate. In order to make the system completely automated, we intend to use deep learning techniques (97, 98). This will reduce the computational steps like feature extraction, ranking and classification. Such systems can be developed using large number of images. Also, small portable IRT camera can also be explored to reduce the cost of the system. This may necessitate ~~to modify~~ modifying our developed algorithm to obtain higher performance as the resolution of the image changes.

5. CONCLUSION

Diabetic foot is a major complication that causes disability, impairs the quality of life and even premature death. An early detection and proper treatment can avoid such overwhelming consequences. In this study, an automated system for early detection of diabetic foot (with and without neuropathy) is developed using DD-DT-CWT coupled with LSDA using left, right and both foot is proposed. The decomposed DD-DT-CWT coefficients are able to depict the subtle variations according to the physiology of the disease. These minute contrast are faithfully captured by the features. Our developed system achieved 93.16% accuracy, 90.91% sensitivity and 98.04% specificity using *four* LSDA features for both foot thermograms with kNN classifier. The developed system can be employed in diabetic clinics, mass diabetes screening and can be used in third world countries where there ~~is~~ are shortages of podiatrist. In future, we intend to ~~develop~~ focus on early detection of ~~diabetes~~ diabetic foot with and with neuropathy ~~foot~~ which can help to prevent ~~the~~ amputation and improve the quality of life. The performance of the work can be improved using better image processing algorithms, and large diverse database.

REFERENCES

1. Organization WH. Definition, diagnosis and classification of diabetes mellitus and its complications: report of a WHO consultation. Part 1, Diagnosis and classification of diabetes mellitus. 1999.
2. Organization WH. Global report on diabetes: World Health Organization; 2016.
3. Amin N, Doupis J. Diabetic foot disease: from the evaluation of the "foot at risk" to the novel diabetic ulcer treatment modalities. World journal of diabetes. 2016;7(7):153.
4. Singh N, Armstrong DG, Lipsky BA. Preventing foot ulcers in patients with diabetes. Jama. 2005;293(2):217-28.
5. Boulton AJ, Kirsner RS, Vileikyte L. Neuropathic diabetic foot ulcers. New England Journal of Medicine. 2004;351(1):48-55.
6. Reiber GE, Vileikyte L, Boyko Ed, Del Aguila M, Smith DG, Lavery LA, et al. Causal pathways for incident lower-extremity ulcers in patients with diabetes from two settings. Diabetes care. 1999;22(1):157-62.
7. Boyko EJ, Ahroni JH, Stensel V, Forsberg RC, Davignon DR, Smith DG. A prospective study of risk factors for diabetic foot ulcer. The Seattle Diabetic Foot Study. Diabetes care. 1999;22(7):1036-42.
8. Abbott C, Carrington A, Ashe H, Bath S, Every L, Griffiths J, et al. The North-West Diabetes Foot Care Study: incidence of, and risk factors for, new diabetic foot ulceration in a community-based patient cohort. Diabetic medicine. 2002;19(5):377-84.
9. Pecoraro RE, Reiber GE, Burgess EM. Pathways to diabetic limb amputation: basis for prevention. Diabetes care. 1990;13(5):513-21.
10. Gilman S. Neurobiology of disease: Academic Press; 2011.
11. Jones BF. A reappraisal of the use of infrared thermal image analysis in medicine. IEEE transactions on medical imaging. 1998;17(6):1019-27.

12. Biederman-Thorson MA, Schmidt RF, Thews G. Human Physiology: Springer Science & Business Media; 2013.

13. Gatt A, Formosa C, Cassar K, Camilleri KP, De Raffaele C, Mizzi A, et al. Thermographic patterns of the upper and lower limbs: baseline data. International journal of vascular medicine. 2015;2015.

14. Hernandez-Contreras D, Peregrina-Barreto H, Rangel-Magdaleno J, Orihuela-Espina F, Ramirez-Cortes J, editors. Measuring changes in the plantar temperature distribution in diabetic patients. Instrumentation and Measurement Technology Conference (I2MTC), 2017 IEEE International; 2017: IEEE.

15. Armstrong DG, Lavery LA, Liswood PJ, Todd WF, Tredwell JA. Infrared dermal thermometry for the high-risk diabetic foot. Physical Therapy. 1997;77(2):169-75.

16. Armstrong DG, Holtz-Neiderer K, Wendel C, Mohler MJ, Kimbriel HR, Lavery LA. Skin temperature monitoring reduces the risk for diabetic foot ulceration in high-risk patients. The American journal of medicine. 2007;120(12):1042-6.

17. Lavery LA, Higgins KR, Lanctot DR, Constantinides GP, Zamorano RG, Armstrong DG, et al. Home monitoring of foot skin temperatures to prevent ulceration. Diabetes care. 2004;27(11):2642-7.

18. Lavery LA, Higgins KR, Lanctot DR, Constantinides GP, Zamorano RG, Athanasiou KA, et al. Preventing diabetic foot ulcer recurrence in high-risk patients. Diabetes care. 2007;30(1):14-20.

19. Stess RM, Sisney PC, Moss KM, Graf PM, Louie KS, Gooding GA, et al. Use of liquid crystal thermography in the evaluation of the diabetic foot. Diabetes care. 1986;9(3):267-72.

20. Chan AW, MacFarlane IA, Bowsher DR. Contact thermography of painful diabetic neuropathic foot. Diabetes Care. 1991;14(10):918-22.

21. Benbow SJ, Chan AW, Bowsher DR, Williams G, Macfarlane IA. The prediction of diabetic neuropathic plantar foot ulceration by liquid-crystal contact thermography. Diabetes care. 1994;17(8):835-9.

22. Lahiri B, Bagavathiappan S, Jayakumar T, Philip J. Medical applications of infrared thermography: a review. Infrared Physics & Technology. 2012;55(4):221-35.

23. Ring F. Thermal imaging today and its relevance to diabetes. SAGE Publications; 2010.

24. Etehadtavakol M, Ng EY. Assessment of Foot Complications in Diabetic Patients Using Thermography: A Review. Application of Infrared to Biomedical Sciences: Springer; 2017. p. 33-43.

25. Hernandez-Contreras D, Peregrina-Barreto H, Rangel-Magdaleno J, Gonzalez-Bernal J. Narrative review: Diabetic foot and infrared thermography. Infrared Physics & Technology. 2016;78:105-17.

26. Ammer K, Melnizky P, Rathkolb O, Ring EF, editors. Thermal imaging of skin changes on the feet of type II diabetics. 2001 Conference Proceedings of the 23rd Annual International Conference of the IEEE Engineering in Medicine and Biology Society; 2001 2001.

27. Melnizky P, Ammer K, Rathkolb O. Thermographic findings of the lower extremity in Patients with Type II diabetes. Thermol int. 2002;12:107-14.

28. Sun P-C, Jao S-HE, Cheng C-K. Assessing foot temperature using infrared thermography. Foot & ankle international. 2005;26(10):847-53.

29. Sun PC, Lin HD, Jao SH, Ku YC, Chan RC, Cheng CK. Relationship of skin temperature to sympathetic dysfunction in diabetic at-risk feet. Diabetes Res Clin Pract. 2006;73(1):41-6.

30. Sun PC, Lin HD, Jao SH, Chan RC, Kao MJ, Cheng CK. Thermoregulatory sudomotor dysfunction and diabetic neuropathy develop in parallel in at-risk feet. Diabet Med. 2008;25(4):413-8.

31. Nishide K, Nagase T, Oba M, Oe M, Ohashi Y, Iizaka S, et al. Ultrasonographic and thermographic screening for latent inflammation in diabetic foot callus. Diabetes Res Clin Pract. 2009;85(3):304-9.

32. Bharara M, Schoess J, Nouvong A, Armstrong DG. Wound Inflammatory Index: A "Proof of Concept" Study to Assess Wound Healing Trajectory. Journal of Diabetes Science and Technology. 2010;4(4):773-9.

33. Bagavathiappan S, Philip J, Jayakumar T, Raj B, Rao PNS, Varalakshmi M, et al. Correlation between Plantar Foot Temperature and Diabetic Neuropathy: A Case Study by Using an Infrared Thermal Imaging Technique. Journal of Diabetes Science and Technology. 2010;4(6):1386-92.

34. Harding J, Wertheim D, Williams R, Melhuish J, Banerjee D, Harding K, editors. Infrared imaging in diabetic foot ulceration. Engineering in Medicine and Biology Society, 1998 Proceedings of the 20th Annual International Conference of the IEEE; 1998: IEEE.

35. Kaabouch N, Chen Y, Anderson JW, Ames F, Paulson R, editors. Asymmetry analysis based on genetic algorithms for the prediction of foot ulcers. VDA; 2009.

36. Kaabouch N, Chen Y, Hu W-C, Anderson J, Ames F, Paulson R, editors. Early detection of foot ulcers through asymmetry analysis. Proc SPIE; 2009.

37. Kaabouch N, Hu W-C, Chen Y, Anderson JW, Ames F, Paulson R. Predicting neuropathic ulceration: analysis of static temperature distributions in thermal images. Journal of biomedical optics. 2010;15(6):061715--6.

38. Kaabouch N, Chen Y, Hu W-C, Anderson JW, Ames F, Paulson R. Enhancement of the asymmetry-based overlapping analysis through features extraction. Journal of Electronic Imaging. 2011;20(1):013012--7.

39. Kaabouch N, Hu W-C, Chen Y. Alternative technique to asymmetry analysis-based overlapping for foot ulcer examination: Scalable scanning. arXiv preprint arXiv:160603578. 2016.

40. Liu C, van der Heijden F, Klein ME, van Baal JG, Bus SA, van Netten JJ. Infrared dermal thermography on diabetic feet soles to predict ulcerations: a case study. 2013.

41. Peregrina-Barreto H, Morales-Hernández L, Rangel-Magdaleno J, Vázquez-Rodríguez P, editors. Thermal image processing for quantitative determination of temperature variations in plantar angiosomes. Instrumentation and Measurement Technology Conference (I2MTC), 2013 IEEE International; 2013: IEEE.

42. van Netten JJ, van Baal JG, Liu C, van Der Heijden F, Bus SA. Infrared thermal imaging for automated detection of diabetic foot complications. SAGE Publications Sage CA: Los Angeles, CA; 2013.

43. Peregrina-Barreto H, Morales-Hernandez LA, Rangel-Magdaleno J, Avina-Cervantes JG, Ramirez-Cortes JM, Morales-Caporal R. Quantitative estimation of temperature variations in plantar angiosomes: a study case for diabetic foot. Computational and mathematical methods in medicine. 2014;2014.

44. van Netten JJ, Prijs M, van Baal JG, Liu C, van Der Heijden F, Bus SA. Diagnostic values for skin temperature assessment to detect diabetes-related foot complications. Diabetes technology & therapeutics. 2014;16(11):714-21.

45. Vilcahuaman L, Harba R, Canals R, Zequera M, Wilches C, Arista M, et al., editors. Detection of diabetic foot hyperthermia by infrared imaging. Engineering in Medicine and Biology Society (EMBC), 2014 36th Annual International Conference of the IEEE; 2014: IEEE.

46. Vilcahuaman L, Harba R, Canals R, Zequera M, Wilches C, Arista M, et al., editors. Automatic Analysis of Plantar Foot Thermal Images in at-Risk Type II Diabetes by Using an Infrared Camera. World Congress on Medical Physics and Biomedical Engineering, June 7-12, 2015, Toronto, Canada; 2015: Springer.

47. Liu C, van Netten JJ, Van Baal JG, Bus SA, van Der Heijden F. Automatic detection of diabetic foot complications with infrared thermography by asymmetric analysis. Journal of biomedical optics. 2015;20(2):026003-.

48. Brånemark P-I, Fagerberg S-E, Langer L, Säve-Söderbergh J. Infrared thermography in diabetes mellitus a preliminary study. Diabetologia. 1967;3(6):529-32.

49. Nagase T, Sanada H, Takehara K, Oe M, Iizaka S, Ohashi Y, et al. Variations of plantar thermographic patterns in normal controls and non-ulcer diabetic patients: novel classification using angiosome concept. Journal of Plastic, reconstructive & aesthetic Surgery. 2011;64(7):860-6.

50. Oe M, Yotsu R, Sanada H, Nagase T, Tamaki T. Screening for osteomyelitis using thermography in patients with diabetic foot. Ulcers. 2013;2013.

51. Bharara M, Boulger E, Grewal GS, Schoess JN, Armstrong DG, editors. Applications of angiosome classification model for monitoring disease progression in the diabetic feet. Proceedings of the 2014 Summer Simulation Multiconference; 2014: Society for Computer Simulation International.

52. Hernandez-Contreras D, Peregrina-Barreto H, Rangel-Magdaleno J, Ramirez-Cortes J, Renero-Carrillo F, Avina-Cervantes G, editors. Evaluation of thermal patterns and distribution applied to the study of diabetic foot. 2015 IEEE International Instrumentation and Measurement Technology Conference (I2MTC) Proceedings; 2015

.

53. Hernandez-Contreras D, Peregrina-Barreto H, Rangel-Magdaleno J, Ramirez-Cortes J, Renero-Carrillo F. Automatic classification of thermal patterns in diabetic foot based on morphological pattern spectrum. Infrared Physics & Technology. 2015;73:149-57.

54. Fushimi H, Inoue T, Yamada Y, Matsuyama Y, Kubo M, Kameyama M. Abnormal vasoreaction of peripheral arteries to cold stimulus of both hands in diabetics. Diabetes research and clinical practice. 1996;32(1-2):55-9.

55. Fujiwara Y, Inukai T, Aso Y, Takemura Y. Thermographic measurement of skin temperature recovery time of extremities in patients with type 2 diabetes mellitus. Experimental and clinical endocrinology & diabetes. 2000;108(07):463-9.

56. Hosaki Y, Mitsunobu F, Ashida K, Tsugeno H, Okamoto M, Nishida N, et al. Non-invasive study for peripheral circulation in patients with diabetes mellitus. 岡大三朝分院研究報告. 2002;72:31-7.

57. Balbinot LF, Canani LH, Robinson CC, Achaval M, Zaro MA. Plantar thermography is useful in the early diagnosis of diabetic neuropathy. Clinics. 2012;67(12):1419-25.

58. Barriga ES, Chekh V, Carranza C, Burge MR, Edwards A, McGrew E, et al., editors. Computational basis for risk stratification of peripheral neuropathy from thermal imaging. Engineering in Medicine and Biology Society (EMBC), 2012 Annual International Conference of the IEEE; 2012: IEEE.

59. Najafi B, Wrobel JS, Grewal G, Menzies RA, Talal TK, Zirie M, et al. Plantar temperature response to walking in diabetes with and without acute Charcot: the Charcot Activity Response Test. Journal of aging research. 2012;2012.

60. Balbinot LF, Robinson CC, Achaval M, Zaro MA, Brioschi ML. Repeatability of infrared plantar thermography in diabetes patients: a pilot study. SAGE Publications Sage CA: Los Angeles, CA; 2013.

61. Yavuz M, Brem RW, Davis BL, Patel J, Osbourne A, Matassini MR, et al. Temperature as a predictive tool for plantar triaxial loading. Journal of biomechanics. 2014;47(15):3767-70.

62. Mori T, Nagase T, Takehara K, Oe M, Ohashi Y, Amemiya A, et al. Morphological pattern classification system for plantar thermography of patients with diabetes. SAGE Publications Sage CA: Los Angeles, CA; 2013.

63. Agurto C, Barriga S, Burge M, Soliz P, editors. Characterization of diabetic peripheral neuropathy in infrared video sequences using independent component analysis. Machine Learning for Signal Processing (MLSP), 2015 IEEE 25th International Workshop on; 2015: IEEE.

64. Tan JH, Ng E, Acharya UR. Evaluation of tear evaporation from ocular surface by functional infrared thermography. Medical physics. 2010;37(11):6022-34.

65. Selesnick IW. The double-density dual-tree DWT. IEEE Transactions on signal processing. 2004;52(5):1304-14.

66. Baradarani A, Wu QJ, Ahmadi M. An efficient illumination invariant face recognition framework via illumination enhancement and DD-DTCWT filtering. Pattern Recognition. 2013;46(1):57-72.

67. Selesnick IW, Baraniuk RG, Kingsbury NC. The dual-tree complex wavelet transform. IEEE signal processing magazine. 2005;22(6):123-51.

68. Hu M-K. Visual pattern recognition by moment invariants. IRE transactions on information theory. 1962;8(2):179-87.

69. Haralick RM, Shanmugam K. Textural features for image classification. IEEE Transactions on systems, man, and cybernetics. 1973(6):610-21.

70. Singh AP, Singh B. Texture features extraction in mammograms using non-shannon entropies. Machine learning and systems engineering: Springer; 2010. p. 341-51.

71. Pharwaha APS, Singh B, editors. Shannon and non-shannon measures of entropy for statistical texture feature extraction in digitized mammograms. proceedings of the World Congress on Engineering and Computer Science; 2009.

72. Karmeshu. Entropy measures, maximum entropy principle and emerging applications: Springer Science & Business Media; 2003.

73. Singh VP. Entropy theory and its application in environmental and water engineering: John Wiley & Sons; 2013.

74. Hu Q, Yu D. Entropies of fuzzy indiscernibility relation and its operations. International Journal of uncertainty, fuzziness and knowledge-based systems. 2004;12(05):575-89.

75. Hung WL, Yang MS. Fuzzy entropy on intuitionistic fuzzy sets. International Journal of Intelligent Systems. 2006;21(4):443-51.

76. Darbellay GA, Vajda I. Entropy expressions for multivariate continuous distributions. IEEE Transactions on Information Theory. 2000;46(2):709-12.

77. Acharya UR, Raghavendra U, Fujita H, Hagiwara Y, Koh JE, Hong TJ, et al. Automated characterization of fatty liver disease and cirrhosis using curvelet transform and entropy features extracted from ultrasound images. Computers in biology and medicine. 2016;79:250-8.

78. Raghavendra U, Acharya UR, Fujita H, Gudigar A, Tan JH, Chokkadi S. Application of Gabor wavelet and Locality Sensitive Discriminant Analysis for automated identification of breast cancer using digitized mammogram images. Applied Soft Computing. 2016;46:151-61.

79. Roweis ST, Saul LK. Nonlinear dimensionality reduction by locally linear embedding. science. 2000;290(5500):2323-6.

80. He X, Cai D, Yan S, Zhang H-J, editors. Neighborhood preserving embedding. Computer Vision, 2005 ICCV 2005 Tenth IEEE International Conference on; 2005: IEEE.

81. He X, Niyogi P, editors. Locality preserving projections. Advances in neural information processing systems; 2004.

82. Cai D, He X, Zhou K, Han J, Bao H, editors. Locality Sensitive Discriminant Analysis. IJCAI; 2007.

83. Stork DG, Duda RO, Hart PE, Stork D. Pattern classification. A Wiley-Interscience Publication. 2001.

84. Schölkopf B, Smola A, Müller K-R. Nonlinear component analysis as a kernel eigenvalue problem. Neural computation. 1998;10(5):1299-319.

85. Verma B, Zhang P. A novel neural-genetic algorithm to find the most significant combination of features in digital mammograms. Applied soft computing. 2007;7(2):612-25.

86. Gelman A. Analysis of variance—why it is more important than ever. The annals of statistics. 2005;33(1):1-53.

87. Faust O, Acharya UR, Ng E, Hong TJ, Yu W. Application of infrared thermography in computer aided diagnosis. Infrared Physics & Technology. 2014;66:160-75.

88. Mosteller F. A k-sample slippage test for an extreme population. Selected Papers of Frederick Mosteller: Springer; 2006. p. 101-9.

89. Larose DT. Discovering knowledge in data: an introduction to data mining: John Wiley & Sons; 2014.

90. Lin W-C, Ke S-W, Tsai C-F. CANN: An intrusion detection system based on combining cluster centers and nearest neighbors. Knowledge-based systems. 2015;78:13-21.

91. Huang Z-H, Li W-J, Wang J, Zhang T. Face recognition based on pixel-level and feature-level fusion of the top-level's wavelet sub-bands. Information Fusion. 2015;22:95-104.

92. Khan A, Farooq H. Principal component analysis-linear discriminant analysis feature extractor for pattern recognition. arXiv preprint arXiv:12041177. 2012.

93. Han J, Kamber M, Pei J. Data mining: concepts and techniques (the Morgan Kaufmann Series in data management systems). Morgan Kaufmann. 2000.

94. Muller K-R, Mika S, Ratsch G, Tsuda K, Scholkopf B. An introduction to kernel-based learning algorithms. IEEE transactions on neural networks. 2001;12(2):181-201.

95. Adam M, Ng EY, Oh SL, Heng ML, Hagiwara Y, Tan JH, et al. Automated characterization of diabetic foot using nonlinear features extracted from thermograms. Infrared Physics & Technology. 2018;89:325-37.

96. Raghavendra U, Fujita H, Gudigar A, Shetty R, Nayak K, Pai U, et al. Automated technique for coronary artery disease characterization and classification using DD-DTDWT in ultrasound images. Biomedical Signal Processing and Control. 2018;40:324-34.

97. Tan JH, Fujita H, Sivaprasad S, Bhandary SV, Rao AK, Chua KC, et al. Automated segmentation of exudates, haemorrhages, microaneurysms using single convolutional neural network. Information Sciences. 2017;420:66-76.

98. Tan JH, Acharya UR, Bhandary SV, Chua KC, Sivaprasad S. Segmentation of optic disc, fovea and retinal vasculature using a single convolutional neural network. Journal of Computational Science. 2017;20:70-9.

APPENDIX A

Table 9: Reduced and ranked features of left foot (normal, diabetic with and without neuropathy).

	Normal		Diabetic non neuropathy		Diabetic neuropathy			
	Mean	Standard deviation	Mean	Standard deviation	Mean	Standard deviation	*p*-Value	*F*-Value
LSDA10	-747.1320	96.5424	-693.6698	226.8194	-878.6887	127.7780	0.0000	13.1682
LSDA15	223.6334	251.1007	-2.8235	139.3799	51.3955	213.5647	0.0000	12.9795
LSDA13	-75.2715	144.5723	-214.5900	136.9546	-200.6785	163.1192	0.0000	11.5800
LSDA11	443.9486	48.9392	484.0063	194.3981	358.0690	70.2165	0.0001	10.6114
LSDA12	205.3205	36.4437	257.1279	159.9037	155.3109	152.8169	0.0034	5.9753
LSDA9	1186.5782	293.6939	1332.4455	166.3339	1212.4419	27.5352	0.0090	4.9085
LSDA20	330.8899	103.7242	421.5288	196.2263	450.1567	273.0794	0.0128	4.5313
LSDA8	-985.4773	95.2675	-791.0194	648.2389	-1008.9049	89.6535	0.0209	4.0007
LSDA23	599.5447	386.0054	448.3403	100.5637	471.2461	194.9321	0.0300	3.6176
LSDA21	-616.1989	348.2198	-500.6570	147.7868	-512.3225	190.8385	0.0861	2.5060
LSDA2	148.3246	113.0887	135.2090	13.3250	78.7438	232.6536	0.0916	2.4408
LSDA18	-395.6905	143.4351	-432.3403	205.2912	-320.7281	352.0587	0.1482	1.9418
LSDA3	-1500.4854	72.5590	-1443.8539	257.5333	-1503.4682	47.4289	0.1635	1.8402
LSDA5	-340.6472	201.1924	-397.0340	60.4366	-375.9343	33.5861	0.1741	1.7750
LSDA16	-543.2297	175.8709	-536.6152	129.5217	-595.7162	204.5338	0.3014	1.2121
LSDA1	-273.1491	32.3395	-261.7636	65.3642	-379.8075	697.5106	0.3472	1.0678
LSDA22	436.1737	292.4979	379.8421	115.9431	374.1397	156.8846	0.3530	1.0507
LSDA14	548.3978	34.5406	581.6349	150.1418	584.1751	190.8207	0.3687	1.0064
LSDA19	278.8786	187.2250	216.0895	242.7978	277.4322	302.2918	0.4532	0.7970
LSDA24	1008.3979	129.1468	1006.7751	254.2493	966.6053	225.6735	0.6046	0.5053
LSDA4	891.9701	170.2597	918.6637	102.6266	887.9397	115.8715	0.6105	0.4956
LSDA17	289.2420	196.3897	270.2165	170.6372	248.1044	215.9056	0.6409	0.4466
LSDA27	-341.7914	79.8953	-359.7232	115.5939	-334.6012	197.7705	0.7263	0.3207
LSDA30	-272.1185	40.6010	-255.5798	228.0437	-277.5766	150.0732	0.8151	0.2048
LSDA29	1355.7012	16.4341	1360.0268	189.5233	1373.0815	151.4289	0.8302	0.1863
LSDA7	-249.6626	28.0619	-217.2909	641.8405	-251.3668	13.7404	0.8944	0.1117
LSDA28	732.0752	37.1264	716.4744	259.8565	723.1762	127.8334	0.9006	0.1047
LSDA6	806.7672	56.4175	783.5255	723.6843	803.5683	48.4429	0.9617	0.0391

LSDA26	-104.7430	255.1337	-114.4474	114.7306	-101.7769	172.8328	0.9641	0.0366
LSDA25	330.6352	59.0106	328.7628	154.6464	332.2090	186.1667	0.9945	0.0055

Table 10: Reduced and ranked features of right foot (normal, diabetic with and without neuropathy).

	Normal		**Diabetic non neuropathy**		**Diabetic neuropathy**			
	Mean	**Standard deviation**	**Mean**	**Standard deviation**	**Mean**	**Standard deviation**	***p*-Value**	***F*-Value**
LSDA7	-588.3974	15.2851	-642.6611	92.0497	-498.1602	206.8906	0.0000	12.2046
LSDA17	-1038.5231	115.8736	-1232.5871	273.4684	-1179.2170	237.2484	0.0001	9.9926
LSDA11	-602.8897	59.6680	-628.8000	218.6416	-493.7734	108.4795	0.0001	9.5886
LSDA10	-489.2856	40.4155	-607.7657	155.1106	-475.8153	223.1547	0.0003	8.5459
LSDA13	-45.3896	208.2115	94.7332	200.6417	87.4450	152.3278	0.0011	7.2873
LSDA21	-465.8533	114.8173	-446.5697	128.6127	-309.8708	369.6098	0.0056	5.4259
LSDA9	-217.3954	10.0810	-327.9471	401.6524	-131.4896	254.0109	0.0079	5.0536
LSDA18	-560.1136	137.4598	-651.5857	168.3295	-573.1768	112.3406	0.0126	4.5501
LSDA12	1185.8805	52.5383	1092.3841	231.7832	1122.8938	133.2222	0.0131	4.5005
LSDA15	14.6296	54.0079	-67.0486	345.3077	-73.8530	123.7634	0.0731	2.6763
LSDA3	-192.3148	21.3019	-133.0309	397.8059	-264.6167	279.6547	0.1206	2.1549
LSDA5	331.9690	22.8634	397.9383	358.9916	265.7930	340.7739	0.1287	2.0878
LSDA16	-157.1838	153.5458	-105.9022	202.8473	-69.8900	266.4006	0.1532	1.9075
LSDA25	-985.9833	316.8081	-884.4740	189.2442	-917.8908	140.6197	0.1559	1.8894
LSDA2	-767.7410	324.7262	-833.9121	45.9941	-854.9544	51.2876	0.1612	1.8549
LSDA20	-314.9327	139.4777	-330.3552	191.3876	-424.0101	442.7070	0.1810	1.7351
LSDA14	269.0604	26.7117	235.3986	322.7959	317.4138	140.6014	0.2059	1.6027
LSDA8	-445.2416	22.6747	-469.2346	65.8057	-407.1014	280.8595	0.2555	1.3810
LSDA1	-6.4995	232.0177	40.0289	23.7270	38.6731	31.9850	0.2882	1.2577
LSDA22	764.4069	173.1481	840.7708	120.0858	795.6446	361.9098	0.3421	1.0829
LSDA6	1124.9033	59.5117	1190.1558	322.0818	1174.7867	338.5794	0.4565	0.7895
LSDA24	610.5660	135.2265	636.4737	204.1904	647.9837	146.6076	0.5493	0.6023
LSDA23	-277.0617	257.7467	-318.6552	171.7591	-265.0366	208.2917	0.5833	0.5416
LSDA19	-785.8136	207.3235	-823.8053	214.7912	-797.6097	191.1624	0.7079	0.3465
LSDA29	1307.9973	270.1800	1282.0929	235.5968	1279.2365	248.0933	0.8467	0.1667
LSDA27	323.9137	181.0759	337.5992	122.6022	333.5160	200.3045	0.9325	0.0699
LSDA26	3.3983	240.1273	15.9067	275.2168	21.9028	163.1878	0.9329	0.0695
LSDA30	-1249.5600	254.8567	-1265.8942	169.2978	-1255.0812	126.8152	0.9368	0.0653
LSDA4	-560.7949	19.4191	-550.9008	212.4843	-565.1147	308.1205	0.9560	0.0450

LSDA28	783.3779	149.8909	777.7428	206.7432	792.8088	282.0433	0.9574	0.0436

Table 11: Reduced and ranked features of bilateral foot (normal, diabetic with and without neuropathy).

	Normal		**Diabetic non neuropathy**		**Diabetic neuropathy**			
	Mean	**Standard deviation**	**Mean**	**Standard deviation**	**Mean**	**Standard deviation**	***p*-Value**	***F*-Value**
LSDA7	-549.7015	240.9483	-1391.4142	737.9976	-308.2853	293.6492	0.0000	54.1820
LSDA8	-1256.7979	764.1630	-994.3039	638.6707	-435.0807	385.3298	0.0000	16.5110
LSDA13	3941.6607	886.3602	4663.9216	591.3424	5186.2978	1513.2969	0.0000	14.8897
LSDA14	2608.5591	725.9480	1826.8859	936.6918	2068.8013	1075.1095	0.0004	8.4331
LSDA10	386.5324	308.5775	832.1888	845.7548	251.7814	1081.7156	0.0054	5.4760
LSDA9	-1152.3434	538.6532	-931.3870	1155.0435	-793.5787	252.8577	0.0767	2.6270
LSDA2	-1313.3676	1173.3528	-1697.2854	618.4535	-1566.4653	144.4376	0.1120	2.2320
LSDA5	1192.0745	179.5669	840.5530	2059.5189	1643.5935	2348.6251	0.1476	1.9455
LSDA1	-2919.7368	114.8001	-3018.0226	269.3410	-2577.8495	1858.5804	0.1668	1.8195
LSDA4	-1104.8317	568.3735	-825.0381	1763.3025	-1266.6822	492.6485	0.2204	1.5326
LSDA11	493.0276	286.3132	544.3337	1143.7309	296.2864	446.7335	0.2845	1.2711
LSDA12	-130.6969	817.5049	-294.7369	442.5649	-321.8697	324.1686	0.2997	1.2178
LSDA6	1710.1122	306.2226	1243.8593	2023.1068	1411.5883	1649.5572	0.3064	1.1953
LSDA16	-1254.5647	526.0252	-1373.0045	662.3374	-1426.3893	525.4640	0.3660	1.0140
LSDA15	-405.6073	705.5331	-276.7986	918.3601	-163.0400	1079.2296	0.4651	0.7708
LSDA18	-1012.1894	435.8985	-844.3118	824.5181	-1005.8025	776.0637	0.4833	0.7318
LSDA22	96.6336	1440.1953	-107.4275	695.6439	-108.7734	396.4345	0.5766	0.5533
LSDA17	-148.7930	850.2466	-366.4587	875.4158	-383.5780	1844.5666	0.6099	0.4966
LSDA30	1380.3695	696.1701	1255.1169	1325.4746	1287.0429	300.1285	0.7819	0.2465
LSDA26	-2309.9822	757.0633	-2401.8813	766.3151	-2395.4979	793.3873	0.8260	0.1915
LSDA21	-3219.3643	674.1720	-3326.2506	836.8185	-3265.6180	1090.6184	0.8548	0.1571
LSDA23	-2246.9848	546.2419	-2208.6727	727.0077	-2158.3996	955.9369	0.8634	0.1470
LSDA20	-1756.9293	981.1203	-1703.4510	1095.1473	-1757.1641	478.3090	0.9596	0.0413
LSDA28	-1460.3581	818.1242	-1476.5235	907.3372	-1509.0797	689.1469	0.9644	0.0363
LSDA19	2604.9360	851.5245	2597.1831	883.4995	2559.3186	759.0127	0.9689	0.0316
LSDA24	722.0593	996.5820	743.6097	856.7453	770.2192	876.7958	0.9732	0.0272
LSDA29	1116.9336	820.7951	1085.3555	498.0491	1110.6683	694.5835	0.9794	0.0209
LSDA3	-1197.8037	121.5989	-1200.4226	2246.6860	-1234.7064	74.8590	0.9893	0.0107
LSDA27	-3930.0268	1131.0500	-3920.8789	765.4076	-3898.5026	1154.3123	0.9909	0.0092
LSDA25	1042.3243	584.1744	1024.1681	430.1474	1047.6969	2033.4685	0.9962	0.0038